Journal of Atmospheric and Solar-Terrestrial Physics 146 (2016) 49–57

Contents lists available at ScienceDirect

Journal of Atmospheric and Solar-Terrestrial Physics

journal homepage: www.elsevier.com/locate/jastp

Ionospheric response under the influence of the solar eclipse occurred on 20 March 2015: Importance of autoscaled data and their assimilation for obtaining a reliable modeling of the ionosphere

M. Pietrella *, M. Pezzopane, A. Settimi

Istituto Nazionale di Geofisica e Vulcanologia, via di Vigna Murata 605, 00143 Rome, Italy

ARTICLE INFO

Article history:
Received 24 December 2015
Received in revised form
17 March 2016
Accepted 19 May 2016
Available online 19 May 2016

Keywords:
Solar eclipse
ISP model
IRI model
Ray tracing

ABSTRACT

This paper wants to highlight how the availability of measurements autoscaled at some reference ionospheric stations, and their assimilation by ionospheric models, was of crucial importance in determining, during the solar eclipse conditions occurred on 20 March 2015, a reliable representation of the ionosphere. Even though the solar eclipse falls in the recovery phase of the St. Patrick geomagnetic storm started on 17 March 2015, its influence on the ionospheric plasma seems undeniable. The reference ionospheric stations considered here are those of Rome (41°.8' N, 12°.5' E), and Gibilmanna (37°.9' N, 14°.0' E), Italy. Specifically, in a time interval including that of the eclipse, the electron density profiles autoscaled by the Automatic Real-Time Ionogram Scaler with True-height (ARTIST) system at San Vito (40°.6′ N, 17°.8′ E), Italy, which are here considered as the truth profiles, were compared with both the electron density profiles calculated by the IRI-SIRMUP-Profiles (ISP) model, after assimilating data recorded at Rome and Gibilmanna, and the electron density profiles provided by the IRI-CCIR model. The ISP and IRI-CCIR performances were then evaluated in terms of the root mean square errors made on the whole electron density profiles. The three-dimensional (3-D) electron density mappings of the ionosphere provided by ISP and IRI-CCIR models were also considered as the ionospheric environment by the ray tracing software tool IONORT to calculate quasi-vertical synthesized ionograms over the short radio link San Vito – Brindisi (40°.4′ N, 17°.6′ E), Italy. The corresponding synthesized values of *fo*F2 and *fx*F2, obtained by IONORT-ISP and IONORT-(IRI-CCIR) procedures, were compared with those autoscaled by ARTIST from the vertical ionograms recorded at the truth site of San Vito. Some examples of IONORT-ISP and IONORT-(IRI-CCIR) synthesized ionograms are shown and discussed. Finally, comparisons in terms of *fo*F2 deduced by long-term prediction and nowcasting maps are also shown. The results achieved in this work demonstrate how the assimilation of autoscaled data into the ionospheric models turned out to be valuable in providing a better representation of the ionospheric electron density under very unusual conditions.

1. Introduction

During a solar eclipse event, the solar disk is obscured by the Moon in such manner that the photochemical activity in the ionosphere is subject to a rapid decrease, thus reaching the levels observed during night time. This gives rise to many different physical phenomena which are well described in the extensive literature gathered in the last decades. Several investigations were indeed conducted to study different ionospheric effects caused by solar eclipse conditions: the detection and enhancement of acoustic gravity waves (Frost and Clark, 1973; Šauli et al., 2006, 2007; Koucká Knížová and Mošna, 2011), and induced gravity waves (Chimonas, 1970; Bertin et al., 1977; Chimonas and Hines, 1971; Fritts and Luo, 1993; Altadill et al., 2001, 2004; Zerefos et al., 2007; Gerasopoulos et al., 2008; Manju et al., 2014; Gang et al., 2015); a decrease of total electron content (Salah et al., 1986; Afraimovich et al., 1998; Baran et al., 2003; Jakowski et al., 2008; Krankowski et al., 2008; Le et al., 2008, 2009; Ding et al., 2010; Momani, and Sulaiman, 2011; Kumar et al., 2013); an increase of the top frequency (*ft*Es) of the sporadic E (Es) layer (Es) (Datta, 1972, 1973; Chen et al., 2010; Yadav et al., 2013), but also its decrease (Minnis, 1955; Stoffregen, 1955); a persistence of the Es layer without any variation of the corresponding intensity (Pezzopane et al., 2015); decreases of the critical frequencies of the ordinary mode of propagation

* Corresponding author.
E-mail addresses: marco.pietrella@ingv.it (M. Pietrella), michael.pezzopane@ingv.it (M. Pezzopane), alessandro.settimi@ingv.it (A. Settimi).

http://dx.doi.org/10.1016/j.jastp.2016.05.006
1364-6826/

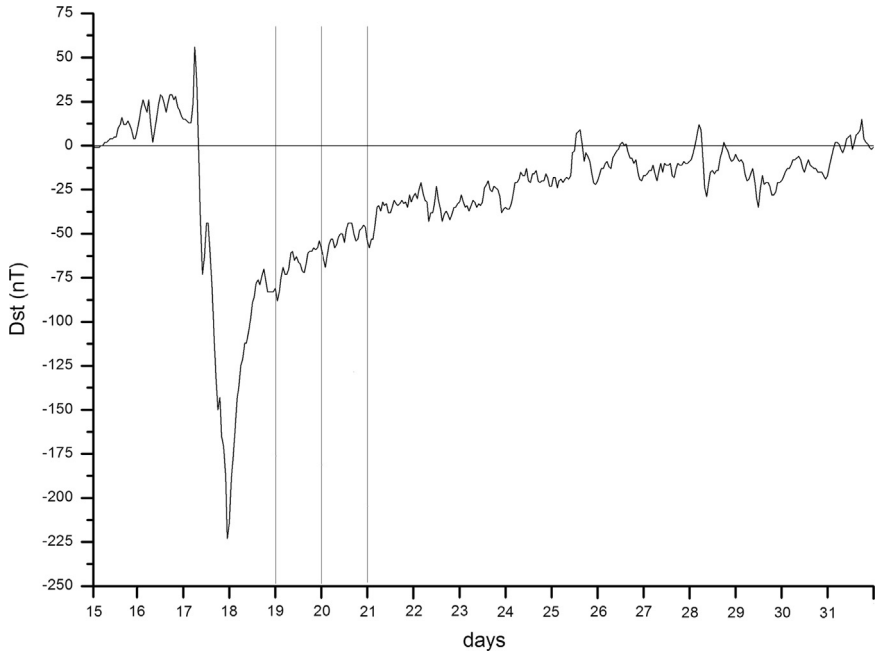

Fig. 1. Dst index recorded from 15 March to 31 March 2015. The three thin vertical lines highlight respectively the day before, during and after the solar eclipse event.

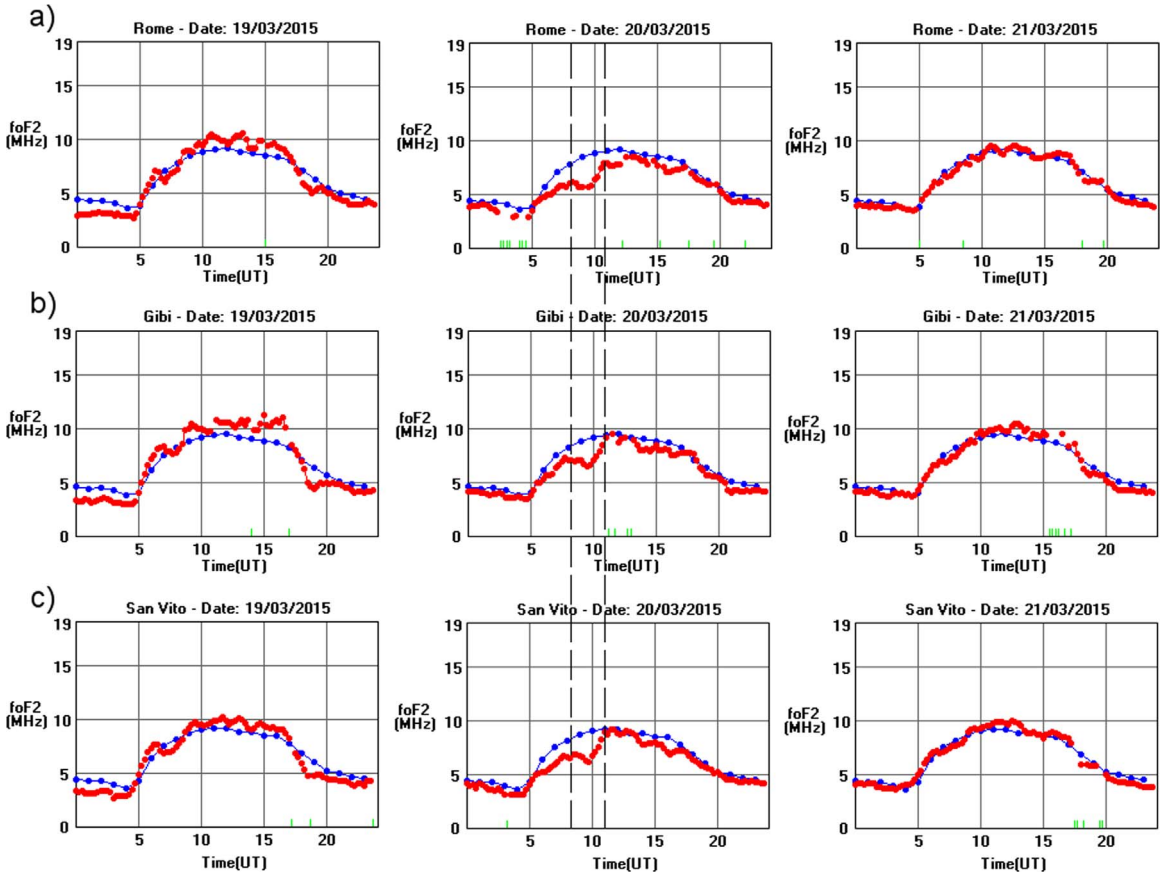

Fig. 2. The *fo*F2 monthly median values predicted by the SIRM long-term prediction model (blue dots) and the *fo*F2 autoscaled values (red dots) for a) Rome, b) Gibilmanna, and c) San Vito, on 19, 20, and 21 March 2015. The dashed vertical lines highlight the start (~08:30 UT) and the end (~10:30 UT) times of the partial solar eclipse occurred on 20 March 2015, as recorded at the ground. The green vertical hyphens that from time to time appear at the bottom of the plots mean that the ionogram was recorded but the autoscaling system did not give any value as output.

*fo*E, *fo*F1, and *fo*F2 of the E, F1, and F2 layers, respectively, (Hunsucker, 1965; Cheng et al., 1992; Adeniyi et al., 2007; Domnin et al., 2013), as well as, albeit rarely, an increase of *fo*F2 (Evans, 1965).

In this investigation *fo*F2 is the characteristic considered to highlight the disturbed ionospheric conditions caused by the solar eclipse event occurred on 20 March 2015. It is worth highlighting that this solar eclipse occurred during the St. Patrick geomagnetic

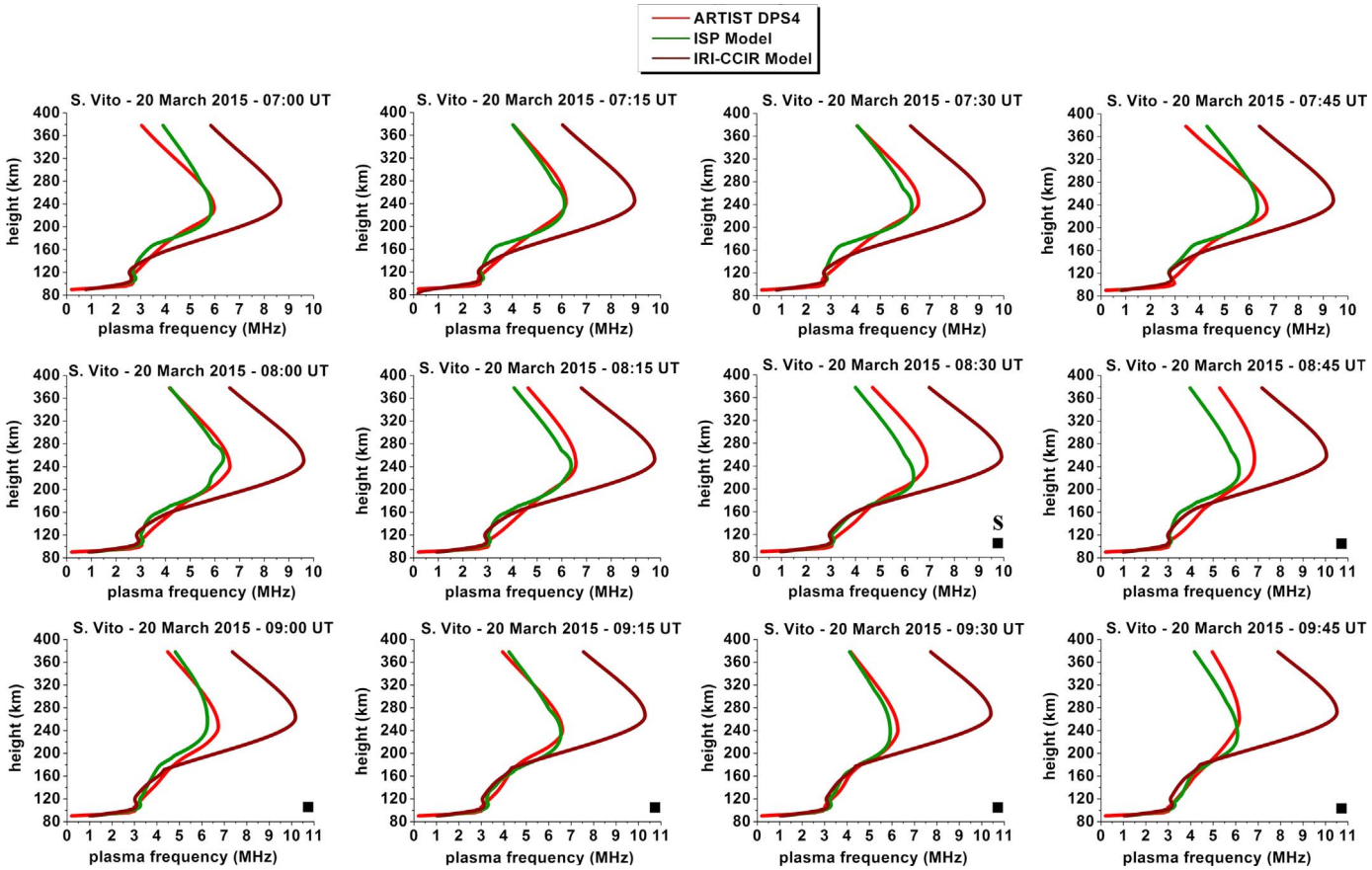

Fig. 3. ISP (in green), IRI-CCIR (in brown), and ARTIST (in red) electron density profiles at the testing-site of San Vito, are shown for the day 20 March 2015 from 07:00 UT to 09:45 UT. The black squares at the right bottom corner of some plots point out the times included in the solar eclipse interval. The letter "s" at 08:30 UT marks the start of the solar eclipse. (For interpretation of the references to color in this figure legend, the reader is referred to the web version of this article.)

storm started on 17 March 2015. With regard to this, Fig. 1 shows the Dst index of the second half of March 2015 by which it is possible to see that the maximum intensity of the storm was reached at around 23:00 UT of 17 March and was characterized by the minimum value of D_{st} index of −223 nT. A detailed description of the complexity characterizing this storm can be found in Cherniak et al. (2015) and Kamide and Kusano (2015).

Under the influence of this storm, *fo*F2 measurements made at Rome (41°.8' N, 12°.5' E, Italy), Gibilmanna (37°.9' N, 14°.0' E, Italy), and San Vito (40°.6′ N, 17°.8′ E, Italy) show deviations from the corresponding monthly median values, which are considered as representative of a quiet state of the ionosphere. However, during the eclipse time window, clear signatures associated to the solar eclipse event are also observed. In fact, even though in Italy the solar eclipse was only partial, with the maximum area of the solar disk obscured by the Moon equal to ∼54% at Rome, ∼45% at Gibilmanna, and ∼47% at San Vito, the *fo*F2 values measured in the corresponding ionospheric stations, in the time interval of the eclipse, between about 08:30 and 10:30 UT, are well below the *fo*F2 monthly median values. Therefore, most likely, besides the geomagnetic storm also the eclipse phenomenon contributes to move significantly away the ionosphere from its usual long-term trend. This study is carried out by considering Rome and Gibilmanna as reference stations, while the ionospheric station of San Vito is considered as the truth-station.

This paper is primarily focused on showing how the assimilation of autoscaled values at some reference ionospheric stations can improve the ionospheric modeling made by long-term models. Specifically, it will be demonstrated that, during the eclipse time, the IRI-SIRMUP-Profiles (ISP) (Pezzopane et al., 2011, 2013) model, and the Simplified Ionospheric Regional Model Updated (SIRMUP) (Zolesi et al., 2004; Tsagouri et al., 2005) model, allow a representation of the ionosphere more reliable than that provided respectively by International Reference Ionosphere (IRI) (Bilitza and Reinisch, 2008) and Simplified Ionospheric Regional Model (SIRM) (Zolesi et al., 1996) long-term prediction models. In order to accomplish this task, the following analysis were carried out:

a) the electron density profiles autoscaled by the Automatic Real-Time Ionogram Scaler with True-height (ARTIST) system (Reinisch and Huang., 1983; Reinisch et al., 2005; Galkin and Reinisch, 2008), assumed as the measured electron density profiles, were compared with the electron density profiles computed by the ISP and the IRI-CCIR models in the truth-station of San Vito;
b) the ISP and IRI-CCIR performances were compared in terms of the root mean square error (r.m.s.e.) calculated over the whole electron density profiles obtained at San Vito;
c) the three-dimensional (3-D) electron density representations of the ionosphere calculated by ISP and IRI-CCIR models were considered by the ray tracing software tool IONORT (IONOspheric Ray-Tracing) (Azzarone et al., 2012) to synthesize quasi-vertical ionograms over the short radio link San Vito - Brindisi (40°.4′ N, 17°.6′ E, Italy), that were compared with those recorded by the DPS4 digisonde (Bibl and Reinisch, 1978) installed at San Vito;
d) *fo*F2 values from the long-term and nowcasting maps generated respectively by the SIRM and SIRMUP models

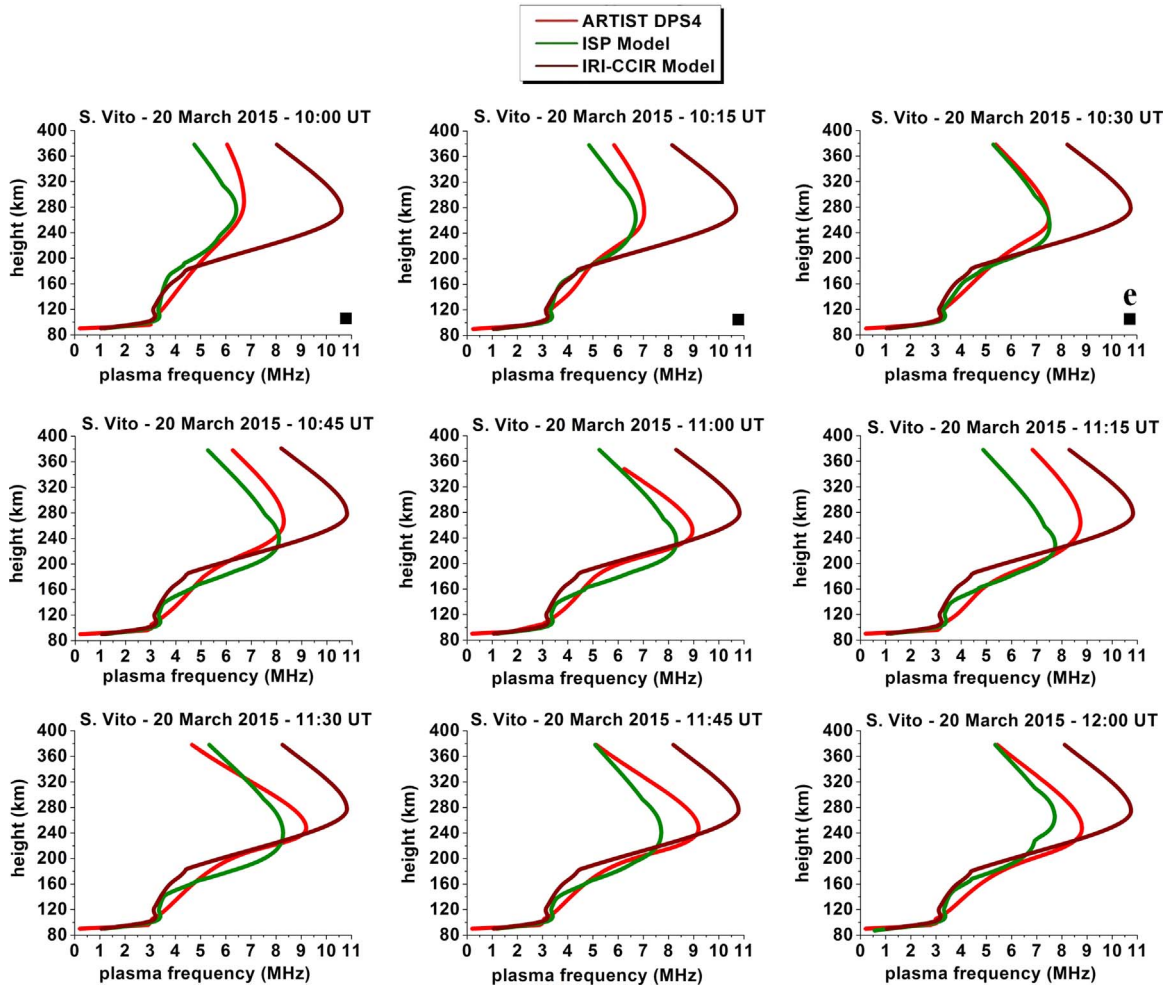

Fig. 4. Same as Fig. 3 but for the time interval 10:00–12:00 UT. The letter "e" at 10:30 UT marks the end of the solar eclipse.

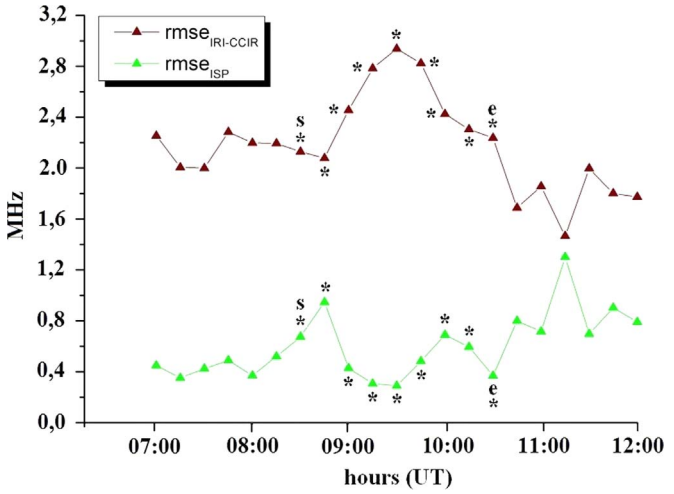

Fig. 5. The values of $rmse_{IRI\text{-}CCIR}$ and $rmse_{ISP}$ calculated in the truth-station of San Vito are shown for the time interval 07:00-12:00 UT. The symbol * labels the times of the solar eclipse. The letters "s" and "e" mark the start and the end of the solar eclipse.

were compared for some hours included in the eclipse time.

The data analysis, the comparisons and the results are presented in Section 2. The discussion of the results is given in Section 3, while a short summary is the subject of Section 4.

2. Data analysis and results

Fig. 2 shows the *fo*F2 monthly median values predicted by the SIRM long-term prediction model (blue dots) and the *fo*F2 autoscaled values (red dots) for Rome (Fig. 1a), Gibilmanna (Fig. 1b), and San Vito (Fig. 1c), on 19 (the day before the solar eclipse), 20 (the solar eclipse day), and 21 (the day after the solar eclipse) March 2015. Specifically, at Rome and Gibilmanna the ionograms were recorded by the AIS-INGV ionosonde (Zuccheretti et al., 2003) and autoscaled by the Autoscala system (Pezzopane and Scotto, 2005, 2007; Scotto, 2009), while at San Vito the ionograms were recorded by the DPS4 digisonde and autoscaled by ARTIST.

Looking at the results of Fig. 2, the day before the solar eclipse event, i.e. on 19 March 2015, during the daytime, the *fo*F2 measurements lie above the monthly median trend. This positive phase is observed until about 18:00 UT when the trend is reversed and a negative phase occurs. The positive and negative deviations of *fo*F2 from the monthly median values are in all likelihood the effects of the St. Patrick storm, they indicate that the ionospheric F2 layer is not quiet but is in some extent perturbed.

The negative phase is observed also the next day, i.e. on 20 March 2015, but in this case the ionosphere is affected not only by the geomagnetic storm but also by the solar eclipse; in fact, during the negative phase, that can be related to the recovery phase of the storm, larger deviations of *fo*F2 from the monthly median trend are observed between the start and end times of the solar eclipse, i.e. between ~08:30 and ~10:30 UT; from 16:00 UT till the end of the day *fo*F2 measured values and long-term values are practically overlapped.

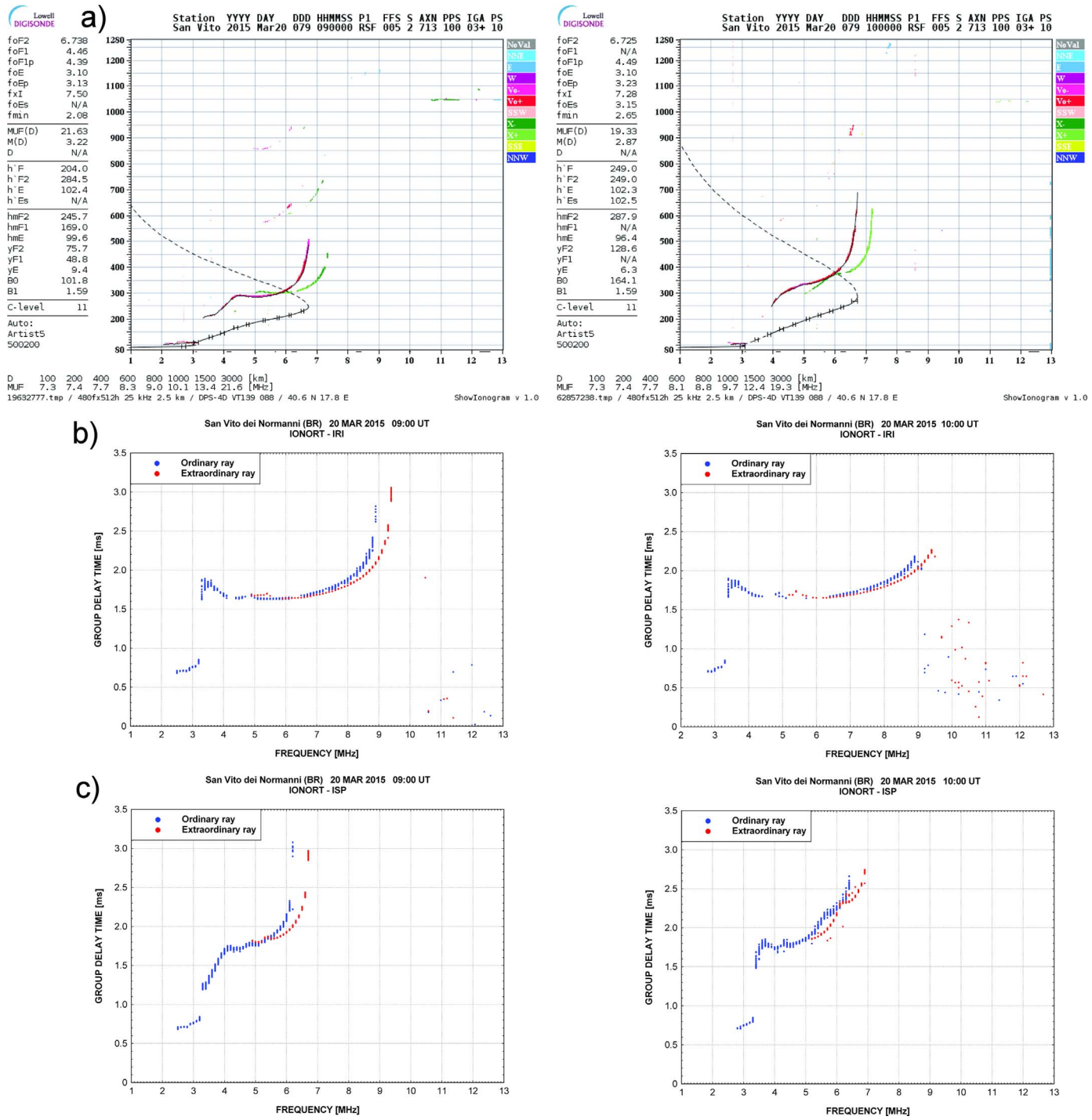

Fig. 6. a) ionograms recorded by the DPS4 digisonde at San Vito on 20 March 2015 at 09:00 UT and 10:00 UT. The corresponding b) IONORT-(IRI-CCIR) and c) IONORT-ISP simulated ionograms, relative to the short radio link San Vito - Brindisi, were computed taking into account both the geomagnetic field provided by the International Geomagnetic Reference Field 12th release (Thébault et al., 2015), and a suitable double exponential profile of electron collision frequency (Settimi et al., 2014). Further details explaining how IONORT works to synthesize ionograms can be found in Settimi et al. (2013, 2015).

The overlapping between measured and long-term *fo*F2 trends continues for the whole 21 March 2015, where no significant positive and negative phases are revealed.

Under the particular ionospheric conditions characterizing the 20 March 2015, in order to obtain a 3-D imaging of the ionosphere as much reliable as possible, a nowcasting model exploiting the autoscaled data should be used. Therefore, in order to improve the ionospheric representation during the eclipse time window, the values of *fo*F2 and the propagation factor *M*(3000)F2, as well as the electron density profiles autoscaled at the reference ionospheric stations of Rome and Gibilmanna, were assimilated by ISP and SIRMUP models, thus obtaining a more reliable mapping of the ionosphere over the southern Italy region.

With regard to this issue, Figs. 3 and 4 show the electron density profiles calculated by the ISP model, by the IRI model with the CCIR option, and those calculated by ARTIST, for the truth-site of San Vito, on 20 March 2015 between 07:00 and 12:00 UT, a time interval including that of the eclipse.

In addition, to evaluate the different performance of the models, the following root mean square errors

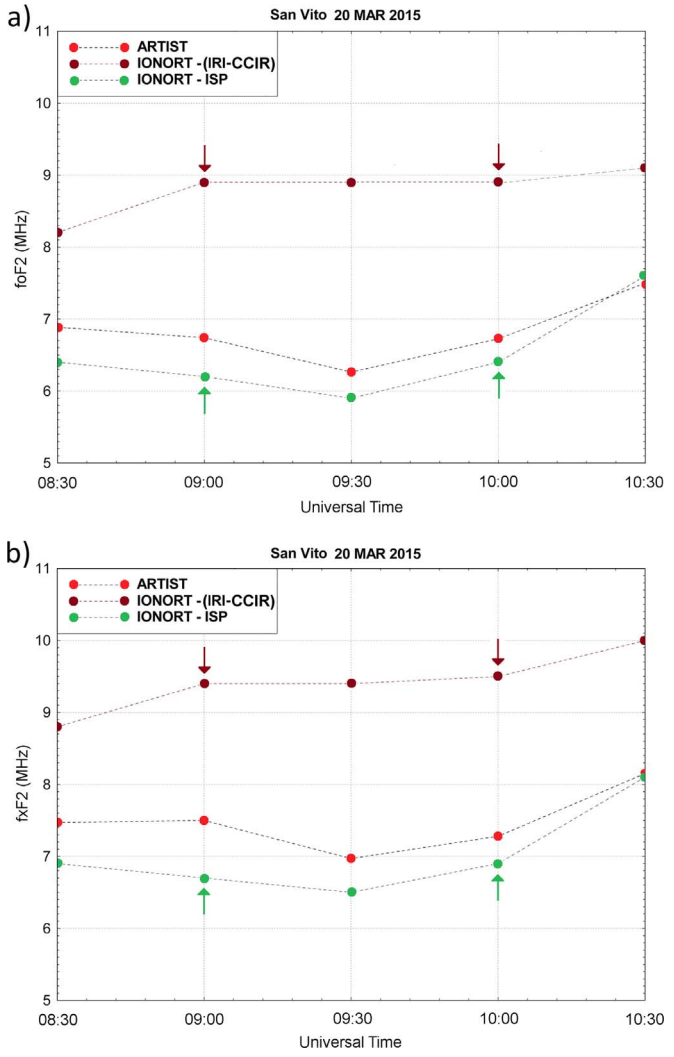

Fig. 7. Comparisons between a) *fo*F2 and b) *fx*F2 inferred from the quasi-vertical ionograms simulated by IONORT-(IRI-CCIR) (brown dots) and IONORT-ISP (green dots) procedures, and measured by ARTIST (red dots) at the truth-site of San Vito, between 08:30 and 10:30 UT on 20 March 2015. The arrows indicate the values of *fo*F2 and *fx*F2 deduced from the simulated quasi vertical ionograms shown in Fig. 6. (For interpretation of the references to color in this figure legend, the reader is referred to the web version of this article.)

$$rmse_{\mathrm{ISP}} = \sqrt{\frac{\sum_{h_{\min}=90\mathrm{km}}^{h_{\max}=378\mathrm{km}} \left(f_{\mathrm{p}}(h)_{\mathrm{ARTIST}} - f_{\mathrm{p}}(h)_{\mathrm{ISP}}\right)^2}{N}} \tag{1a}$$

$$rmse_{\mathrm{IRI-CCIR}} = \sqrt{\frac{\sum_{h_{\min}=90\mathrm{km}}^{h_{\max}=378\mathrm{km}} \left(f_{\mathrm{p}}(h)_{\mathrm{ARTIST}} - f_{\mathrm{p}}(h)_{\mathrm{IRI-CCIR}}\right)^2}{N}} \tag{1b}$$

were calculated at the truth-site of San Vito over the whole electron density profile. In Eq. 1a,b $f_{\mathrm{p}}(h)_{\mathrm{ARTIST}}$ represents the plasma frequency at a definite real height h, autoscaled by the ARTIST system at San Vito, while $f_{\mathrm{p}}(h)_{\mathrm{ISP}}$ and $f_{\mathrm{p}}(h)_{\mathrm{IRI-CCIR}}$, represent respectively the plasma frequencies at a definite real height h modeled by ISP and IRI-CCIR models; N is the number of data.

Hence, the values of $rmse_{\mathrm{ISP}}$ and $rmse_{\mathrm{IRI-CCIR}}$ were calculated and plotted in Fig. 5 for the time interval 07:00–12:00 UT.

The 3-D electron density mappings of the ionosphere calculated by the IRI-CCIR and ISP models, were also used as the ionospheric environment by the software tool IONORT to calculate the ray tracing along the radio link San Vito - Brindisi. As the ground range between San Vito and Brindisi is ~ 28 km, the ionograms synthesized by IONORT-(IRI-CCIR) and IONORT-ISP procedures (see Fig. 6) can be considered as quasi vertical.

For this reason, these ionograms were then compared with the vertical ionograms recorded by the DPS4 digisonde at the truth-station of San Vito during the solar eclipse time interval, between 08:30 and 10:30 UT; the values of *fo*F2 and the critical frequencies of the extraordinary mode of propagation (*fx*F2), deduced from the IONORT-(IRI-CCIR) and IONORT-ISP ionograms, are compared with the *fo*F2 and *fx*F2 values autoscaled by ARTIST which are here assumed as the true measurements. The corresponding results are shown in Fig. 7.

Finally, maps of *fo*F2 layer, generated by SIRM and SIRMUP models on 20 March 2015 at 09:00 UT and 10:00 UT (Fig. 8), were also considered to make further comparisons between long term and nowcasting predictions over San Vito.

3. Discussion of the results

The solar eclipse event under study occurred during the recovery phase of the St. Patrick storm commenced on 17 March 2015 with the arrival at Earth of a coronal mass ejection. During this storm the Dst index reached a minimum value of −223 nT (Fig. 1), while the Kp index reached a maximum value of 8, which classifies the event as a severe geomagnetic storm. Hence, the corresponding effects on the ionosphere cannot be certainly neglected.

In fact, looking at the results of Fig. 2, the day before the solar eclipse event, i.e. on 19 March 2015, during the daytime, the *fo*F2 measurements lie above the monthly median trend. This positive phase is observed until about 18:00 UT when the trend is reversed and a negative phase occurs. These positive and negative departures of *fo*F2 from the monthly median values are most likely due to the effect that the geomagnetic storm has on the ionospheric F2 layer.

The negative phase is observed also the next day, i.e. on 20 March 2015, but in this case, besides the geomagnetic storm, also the solar eclipse event occurred between 08:30 and 10:30 UT is to be considered as an additional physical phenomenon causing the reduction of *fo*F2 with respect to the long term trend values.

With respect to the monthly median trend, a decrease of *fo*F2 is observed before the eclipse start time in all the stations; these reductions, like that of about 2 MHz observed in Rome at 08:00 UT, can be ascribed to the effect of the geomagnetic storm.

However, it is noteworthy to highlight that the solar eclipse occurred right during the recovery phase of the geomagnetic storm (see Fig. 1). As the recovery phase is usually characterized by an abatement of perturbations and a gradual return to the “ground state” of the ionosphere, it is reasonable to attribute most of the decrease of *fo*F2 observed between 08:30 and 10:30 UT (Fig. 2) to the solar eclipse event. In support of this assertion two main aspects can be taken into account:

1) if we focus our attention on the eclipse time interval of Fig. 2, we observe a decreasing trend of *fo*F2 which, after reaching its minimum, starts to increase again following pretty well the usual eclipse transmission factor “shape”;
2) the largest deviations of *fo*F2 from the monthly median values are observed right during the eclipse time, confirming a well-known phenomenon due to the rapid decrease of the photo-ionization process characterizing a solar eclipse (Hunsucker, 1965; Cheng et al., 1992; Adeniyi et al., 2007; Domnin et al., 2013).

A further evidence that the 20 March 2015 solar eclipse affected significantly the ionospheric plasma is the study conducted

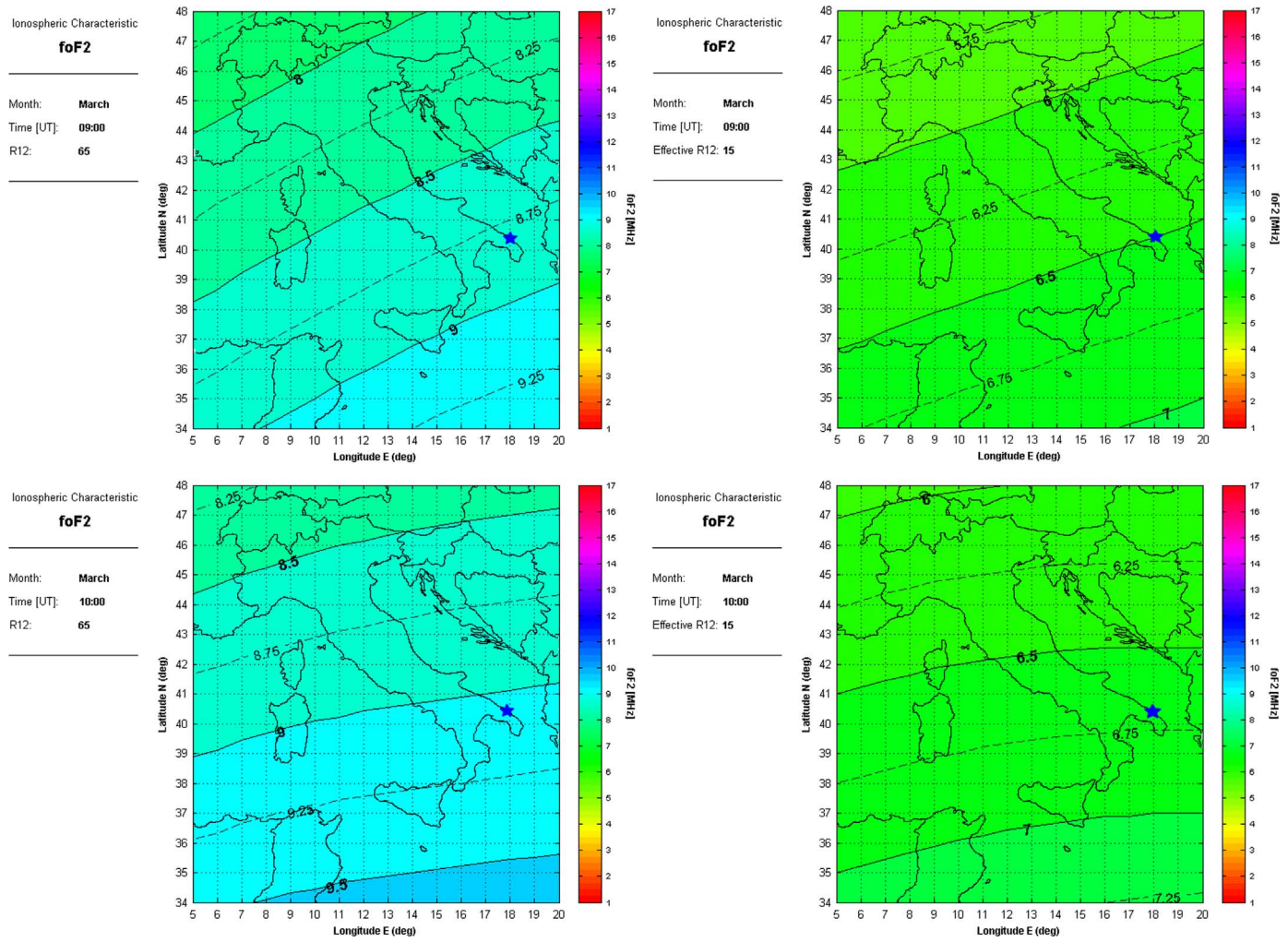

Fig. 8. Maps of *fo*F2 generated by SIRM (left panels) and SIRMUP (right panels) models at 09:00 UT (top panels) and 10:00 UT (bottom panels). The blue star marks the truth-site of San Vito. The effective value of the solar index R_{12} visible on SIRMUP maps was calculated after assimilating the *fo*F2 values recorded at the reference ionospheric stations of Rome and Gibilmanna (Zolesi et al., 2004).

by Pezzopane et al. (2015) where it is clearly shown how the persistency of the Es layer, in the same region considered in this investigation, is strictly linked to the solar eclipse phenomenon.

The day following the solar eclipse event, i.e. on 21 March 2015, the *fo*F2 measurements can be considered practically overlapped on the corresponding long-term trends for all the three stations, thus indicating that the geomagnetic storm has no more influence on the ionosphere.

In the light of the aforementioned considerations, the authors feel that there exist clear ionospheric signatures related to the solar eclipse. That's why the levels of electron density in this "under eclipse" ionosphere are then well below the average values, and therefore they are improperly represented by long-term models.

Our analysis has shown that, if these models are fed with autoscaled data at some reference ionospheric stations, this misrepresentation can be significantly mitigated.

Concerning this, Figs. 3 and 4 clearly show that the ISP procedure after assimilating *fo*F2, *M*(3000)F2, and electron density profiles autoscaled from ionograms recorded in the reference ionospheric stations, provides a 3-D electron density mapping of the ionosphere significantly better than that provided by the IRI-CCIR model, especially during the eclipse time.

From a quantitative point of view, this is also confirmed by the results presented in Fig. 5, where the values of $rmse_{\text{IRI-CCIR}}$, larger than that of $rmse_{\text{ISP}}$, indicate that the ionospheric representation given by the IRI-CCIR model is always worse than that provided by the ISP model. The relatively higher values of $rmse_{\text{IRI-CCIR}}$, with respect to $rmse_{\text{ISP}}$ ones, observed in the central part of Fig. 5, specifically from 09:00 to 09:45 UT, represent a further quantitative verification that in full solar eclipse event, while ISP models quite well the ionospheric plasma, the IRI-CCIR ionospheric modeling is rather poor.

To reinforce this result, the IONORT ray tracing algorithm was run on the 3-D electron density specification of the ionosphere made both by ISP and IRI-CCIR to synthesize quasi-vertical ionograms over the path San Vito – Brindisi, that were compared with those recorded at San Vito.

In fact, from the results of Fig. 7, showing the comparisons between the synthetic values of *fo*F2 and *fx*F2, and those measured, it emerges unequivocally that the IONORT-ISP critical frequencies are by far always more reliable than the IONORT- (IRI-CCIR) ones. This means that the ISP ionospheric environment through which the radio wave travels is more realistic than that given by the IRI-CCIR model

This consideration is a fortiori true looking at Fig. 6, where the shape of the simulated ionograms generated by the IONORT-ISP procedure is more similar to the shape of the ionograms recorded at San Vito, than the shape of the simulated ionograms generated by the IONORT-(IRI-CCIR) procedure.

The importance of the assimilation of autoscaled data, for describing properly the unusual behavior of the ionosphere in the eclipse time window, is also evident when comparing *fo*F2 maps generated by the long term SIRM model and by the nowcasting SIRMUP model, which gives its output after assimilating *fo*F2 values recorded at the reference ionospheric stations of Rome and Gibilmanna.

Fig. 8 shows the maps of *fo*F2, generated on 20 March 2015 at 09:00 UT and 10:00 UT (hence, in full solar eclipse) by SIRM and SIRMUP; from these maps the values of *fo*F2 over the truth-station of San Vito were extrapolated obtaining: 8.75(6.45) MHz at 09:00 UT and 9.01(6.64) MHz at 10:00 UT, for SIRM(SIRMUP). As the *fo*F2 values autoscaled by ARTIST at San Vito are 6.74 at 09:00 and 6.73 MHz at 10:00 UT, it is quite evident that also in this case the SIRM model fails in predicting the values of *fo*F2, while the assimilation of autoscaled data, in this case made by the SIRMUP model, turned out to be valuable to predict satisfactorily the behavior of the ionosphere under the uncommon conditions characterizing the solar eclipse event.

4. Summary

The St. Patrick storm commenced on 17 March 2015 has certainly affected the usual behavior of the ionospheric plasma, nevertheless some ionospheric signatures related to the 20 March 2015 solar eclipse event were also found, even though in the region under investigation the eclipse was only partial. Specifically, during the solar eclipse time window, the ionosphere was so different from its normal state that the long term prediction models such as IRI-CCIR and SIRM could not reliably represent it. All of them forecasted an ionosphere by far different from the real one.

This work represents an additional contribution aimed to show how the availability of autoscaled data recorded at some reference ionospheric stations is of crucial importance for the specification of a “true” ionosphere, especially for conditions like those caused by a solar eclipse.

The assimilation of autoscaled data by long-term models is fundamental to obtain a representation of the ionospheric plasma which is as much accurate and reliable as possible.

Acknowledgements

The authors are very grateful to the unknown referees for their useful comments and suggestions which have greatly contributed to improve the paper.

References

Adeniyi, J.O., Radicella, S.M., Adimula, I.A., Willoughby, A.A., Oladipo, O.A., Olawepo, O., 2007. Signature of the 29 March 2006 eclipse on the ionosphere over an equatorial station. J. Geophys. Res. 112, A06314. http://dx.doi.org/10.1029/2006JA012197.

Afraimovich, E.L., Palamartchouk, K.S., Perevalova, N.P., Chernukhov, V.V., Lukhnev, A.V., Zalutsky, V.T., 1998. Ionospheric effects of the solar eclipse of March 9, 1997, as deduced from GPS data. Geophys. Res. Lett. 25 (4), 465–468. http://dx.doi.org/10.1029/98GL00186.

Altadill, D., Solé, J.G., Apostolov, E., 2001. Vertical structure of a gravity wave like oscillation in the ionosphere generated by the solar eclipse of August 11, 1999. J. Geophys. Res. 106 (A10). http://dx.doi.org/10.1029/2001JA900069.

Altadill, D., Apostolov, E.M., Boska, J., Lastovicka, J., Sauli, P., 2004. Planetary and gravity wave signatures in the *F*-region ionosphere with impact on radio propagation predictions and variability. Ann. Geophys. 47 (2/3). http://dx.doi.org/10.4401/ag-3288.

Azzarone, A., Bianchi, C., Pezzopane, M., Pietrella, M., Scotto, C., Settimi, A., 2012. IONORT: a windows software tool to calculate the HF ray tracing in the ionosphere. Comput. Geosci. 42, 57–63. http://dx.doi.org/10.1016/j.cageo.2012.02.008.

Baran, L.W., Ephishov, I.I., Shagimuratov, I.I., Ivanov, V.P., Lagovsky, A.F., 2003. The response of the ionospheric total electron content to the solar eclipse on August 11, 1999. Adv. Space Res. 31 (4), 989–994.

Bertin, F., Hughes, K.A., Kersley, L., 1977. Atmospheric waves induced by the solar eclipse of 30 June 1973. J. Atmos. Sol. Terr. Phys. 39, 457–461.

Bibl, K., Reinisch, B.W., 1978. The universal digital ionosonde. Radio Sci. 13, 519–530. http://dx.doi.org/10.1029/RS013i003p00519.

Bilitza, D., Reinisch, B.W., 2008. International reference ionosphere 2007: improvements and new parameters. Adv. Space Res. 42 (4), 599–609. http://dx.doi.org/10.1016/j.asr.2007.07.048.

Chen, G., Zhao, Z., Yang, G., Zhou, C., Yao, M., Li, T., Huang, S., Li, N., 2010. Enhancement and HF doppler observations of sporadic-E during the solar eclipse of 22 July 2009. J. Geophys. Res. 115, A09325. http://dx.doi.org/10.1029/2010JA015530.

Cheng, K., Huang, Y.N., Chen, S.W., 1992. Ionospheric effects of the solar eclipse of September 23, 1987, around the equatorial anomaly crest region. J. Geophys. Res. 97 (A1), 103–111. http://dx.doi.org/10.1029/91JA02409.

Cherniak, I., Zakharenkova, I., Redmon, R.J., 2015. Dynamics of the high-latitude ionospheric irregularities during the 17 March 2015 St. Patrick's Day storm: ground-based GPS measurements. Space Weather 13. http://dx.doi.org/10.1002/2015SW001237.

Chimonas, G., 1970. Internal gravity-wave motions induced in the earth's atmosphere by a solar eclipse. J. Geophys. Res. 75 (28), 5545–5551.

Chimonas, G., Hines, C.O., 1971. Atmospheric gravity waves induced by a solar eclipse, 2. J. Geophys. Res. 76 (28), 7003–7005.

Datta, R.N., 1972. Solar-eclipse effect on sporadic-E ionization. J. Geophys. Res. 77 (1), 260–262. http://dx.doi.org/10.1029/JA077i001p00260.

Datta, R.N., 1973. Solar eclipse effect on sporadic E ionization, 2. J. Geophys. Res. 78 (1), 320–322.

Ding, F., Wan, W., Ning, B., Liu, L., Le, H., Xu, G., Wang, M., Li, G., Chen, Y., Ren, Z., et al., 2010. GPS TEC response to the 22 July 2009 total solar eclipse in East Asia. J. Geophys. Res. 115, A07308. http://dx.doi.org/10.1029/2009JA015113.

Domnin, I.F., Yemel'yanov, L., Ya., Kotov, D.V., Lyashenko, M.V., Chernogor, L.F., 2013. Solar eclipse of August 1, 2008, above Kharkov: 1. Results of incoherent scatter observations. Geomagn. Aeron. 53 (1), 113–123. http://dx.doi.org/10.1134/S0016793213010076.

Evans, J.V., 1965. On the behaviour of foF2 during solar eclipses. J. Geophys. Res. 70 (3), 733–738. http://dx.doi.org/10.1029/JZ070i003p00733.

Fritts, D.C., Luo, Z., 1993. Gravity wave forcing in the middle atmosphere due to reduced ozone heating during a solar eclipse. J. Geophys. Res. 98 (D2), 3011–3021. http://dx.doi.org/10.1029/92JD02391.

Frost, A.D., Clark, R.R., 1973. Predicted acoustic gravity wave enhancement during the solar eclipse of June 30. J. Geophys. Res. 78, 3995–3997. http://dx.doi.org/10.1029/JA078i019p03995.

Galkin, I.A., Reinisch, B.W., 2008. The new ARTIST 5 for all Digisondes, in Ionosonde Network Advisory Group Bulletin, in: IPS Radio and Space Serv., Surry Hills, N.S.W., Australia, vol. 69, pp. 1-8. Available at: ⟨http://www.ips.gov.au/IPSHosted/INAG/web-69/2008/artist5-inag.pdf⟩.

Gang, C., Wu., C., Huang, X., Zhao, Z., Zhong, D., Qi, H., Huang, L., Qiao, L., Wang, J., 2015. Plasma flux and gravity waves in the midlatitude ionosphere during the solar eclipse of 20 May 2012. J. Geophys. Res. 120 (4), 3009–3020. http://dx.doi.org/10.1002/2014JA020849.

Gerasopoulos, E., Zerefos, C.S., Tsagouri, I., Founda, D., Amiridis, V., Bais, A.F., Belehaki, A., Christou, N., Economou, G., Kanakidou, M., Karamanos, A., Petrakis, M., Zanis, P., 2008. The total solar eclipse of March 2006: overview. Atmos. Chem. Phys. 8, 5205–5220. http://dx.doi.org/10.5194/acp-8-5205-2008.

Hunsucker, R., 1965. Radio studies of the high-latitude ionosphere during the solar eclipse of 20 July 1963. Radio Sci. 69 (2), 267–272. http://dx.doi.org/10.6028/jres.069D.037.

Jakowski, N., Stankov, S.M., Wilken, V., Borries, C., Altadill, D., Chum, J., Buresova, D., Boska, J., Sauli, P., Hruska, F., Cander, Lj.R., 2008. Ionospheric behavior over Europe during the solar eclipse of 3 October 2005. J. Atmos. Solar Terr. Phys. 70, 836–853.

Kamide, Y., Kusano, K., 2015. No major solar flares but the largest geomagnetic storm in the present solar cycle. Space Weather 13. http://dx.doi.org/10.1002/2015SW001213.

Koucká Knížová, P., Mošna, Z., 2011. Acoustic-gravity waves in the ionosphere during solar eclipse events, in: Marco G. Beghi (Ed.), Acoustic Waves – From Microdevices to Helioseismology, ISBN: 978-953-307-572-3, doi: 10.5772/19722. Available from: ⟨http://www.intechopen.com/books/acoustic-waves-from-microdevices-tohelioseismology/acoustic-gravity-waves-in-the-ionosphere-during-solar-eclipse-events⟩.

Krankowski, A., Shagimuratov, I.I., Baran, L.W., Yakimova, G.A., 2008. The effect of total solar eclipse of October 3, 2005, on the total electron content over Europe. Adv. Space Res. 41, 628–638. http://dx.doi.org/10.1016/j.asr.2007.11.002.

Kumar, S., Singh, A.K., Singh, R.P., 2013. Ionospheric response to total solar eclipse of 22 July 2009 in different Indian regions. Ann. Geophys. 31, 1549–1558. http://dx.doi.org/10.5194/angeo-31-1549-2013.

Le, H., Liu, L., Yue, X., Wan, W., 2008. The ionospheric responses to the 11 August 1999 solar eclipse: Observations and modeling. Ann. Geophys. 26, 107–116. http://dx.doi.org/10.5194/angeo-26-107-2008.

Le, H., Liu, L., Yue, X., Wan, W., Ning, B., 2009. Latitudinal dependence of the ionospheric response to solar eclipse. J. Geophys. Res. 114, A07308. http://dx.doi.org/10.1029/2009JA014072.

Manju, G., Madhav Haridas, M.K., Ramkumar, G., Tarun, K., Pant, Sridharan, R., Sreelatha, P., 2014. Gravity wave signatures in the dip equatorial ionosphere-

thermosphere system during the annular solar eclipse of 15 January 2010. J. Geophys. Res. 119 (6), 4929–4937. http://dx.doi.org/10.1002/2014JA019865.
Minnis, C.M., 1955. Ionospheric behaviour at Khartoum during the eclipse of 25th February 1952. J. Atmos. Terr. Phys. 6, 91–112.
Momani, M.A., Sulaiman, S., 2011. Ionospheric response to the annular solar eclipse on 15th January 2010 as observed by ionosonde receivers. J. Adv. Sci. Eng. Res. 1 (2), 238–245.
Pezzopane, M., Scotto, C., 2005. The INGV software for the automatic scaling of foF2 and MUF(3000)F2 from ionograms: a performance comparison with ARTIST 4.01 from Rome data. J. Atmos. Solar-Terr. Phys. 67 (12), 1063–1073. http://dx.doi.org/10.1016/j.jastp.2005.02.022.
Pezzopane, M., Scotto, C., 2007. The automatic scaling of critical frequency foF2 and MUF(3000)F2: a comparison between Autoscala and ARTIST 4.5 on Rome data. Radio Sci. 42, RS4003. http://dx.doi.org/10.1029/2006RS003581.
Pezzopane, M., Pietrella, M., Pignalberi, A., Tozzi, R., 2015. 20 March 2015 solar eclipse influence on sporadic E layer. Adv. Space Res. 56 (10), 2064–2072. http://dx.doi.org/10.1016/j.asr.2015.08.001.
Pezzopane, M., Pietrella, M., Pignatelli, A., Zolesi, B., Cander, L.R., 2011. Assimilation of autoscaled data and regional and local ionospheric models as input sources for real-time 3-D international reference ionosphere modelling. Radio Sci. 46 (5), RS5009. http://dx.doi.org/10.1029/2011RS004697.
Pezzopane, M., Pietrella, M., Pignatelli, A., Zolesi, B., Cander., L.R., 2013. Testing the three-dimensional IRI-SIRMUP-P mapping of the ionosphere for disturbed periods. Adv. Space Res. 52 (10), 1726–1736. http://dx.doi.org/10.1016/j.asr.2012.11.028.
Reinisch, B.W., Huang., X., 1983. Automatic calculation of electron density profiles from digital ionograms: 3. Processing of bottom side ionograms. Radio Sci. 18 (3). http://dx.doi.org/10.1029/RS018i003p00477.
Reinisch, B.W., Huang, X., Galkin, I.A., Paznukhov, V., Kozlov, A., 2005. Recent advances in real-time analysis of ionograms and ionospheric drift measurements with digisondes. J. Atmos. Solar-Terr. Phys. 67 (12), 1054–1062. http://dx.doi.org/10.1016/j.jastp 2005.01.009.
Salah, J.E., Oliver, W.L., Foster, J.J., Holt, J.M., Emery, B.A., Roble, R.G., 1986. Observation of the May 30, 1984, annular solar eclipse at Millstone Hill. J. Geophys. Res. 91 (A2), 1651–1660.
Šauli, P., Abry, P., Boska, J., Duchayne, L., 2006. Wavelet characterisation of ionospheric acoustic and gravity waves occurring during the solar eclipse of August 11, 1999. J. Atmos. Sol. Terr. Phys. 68 (3-5), 586–598. http://dx.doi.org/10.1016/j.jastp.2005.03.024.
Šauli, P., Roux, S.G., Abry, P., Boska, J., 2007. Acoustic-gravity waves during solar eclipses: Detection and characterization using wavelet transforms. J. Atmos. Sol. Terr. Phys. 69 (17–18), 2465–2484. http://dx.doi.org/10.1016/j.jastp.2007.06.012.
Scotto, C., 2009. Electron Density profile calculation technique for autoscala ionogram analysis. Adv. Space Res. 44, 756–766. http://dx.doi.org/10.1016/j.asr.2009.04.037.
Settimi, A., Pietrella, M., Pezzopane, M., Bianchi, C., 2015. The IONORT-ISP-WC system: inclusion of an electron collision frequency model for the D-layer, in special issue: international reference ionosphere (iri) and global navigation satellite systems (GNSS). Adv. Space Res. 55 (8), 2114–2123. http://dx.doi.org/10.1016/j.asr.2014.07.040.
Settimi, A., Pietrella, M., Pezzopane, M., Zolesi, B., Bianchi, C., Scotto, C., 2014. The COMPLEIK subroutine of the IONORT-ISP system for calculating the non-deviative absorption: a comparison with the ICEPAC formula. Adv. Space Res. 53 (2), 201–218. http://dx.doi.org/10.1016/j.asr.2013.10.035.
Settimi, A., Pezzopane, M., Pietrella, M., Bianchi, C., Scotto, C., Zuccheretti, E., Makris, J., 2013. Testing the IONORT-ISP system: a comparison between synthesized and measured oblique ionograms. Radio Sci. 48 (2), 167–179. http://dx.doi.org/10.1002/rds.20018.
Stoffregen, W., 1955. Variation of fEs during solar eclipses. Nature 176, 610.
Thébault, E., Finlay, C.C., Toh, H., 2015. International geomagnetic reference field – the twelfth generation. Earth Planets Space Spec. Issue 67, 158. http://dx.doi.org/10.1186/s40623-015-0313-0.
Tsagouri, I., Zolesi, B., Belehaki, A., Cander, L.R., 2005. Evaluation of the performance of the real-time updated simplified ionospheric regional model for the European area. J. Atmos. Sol. Terr. Phys. 67 (12), 1137–1146. http://dx.doi.org/10.1016/j.jastp.2005.01.012.
Yadav, S., Das, R.M., Dabas, R.S., Gwal, A.K., 2013. The response of sporadic E-layer to the total solar eclipse of July 22, 2009 over the equatorial ionization anomaly region of the Indian zone. Adv. Space Res. 51 (11), 2043–2047. http://dx.doi.org/10.1016/j.asr.2013.01.011.
Zerefos, C.S., Gerasopoulos, E., Tsagouri, I., Psiloglou, B.E., Belehaki, A., Herekakis, T., Bais, A., Kazadzis, S., Eleftheratos, C., Kalivitis, N., Mihalopoulos, N., 2007. Evidence of gravity waves into the atmosphere during the March 2006 total solar eclipse. Atmos. Chem. Phys. 7, 4943–4951. http://dx.doi.org/10.5194/acp-7-4943-2007.
Zolesi, B., Cander, L.R., De Franceschi, G., 1996. On the potential applicability of the simplified ionospheric regional model to different midlatitude areas. Radio Sci. 31 (3), 547–552. http://dx.doi.org/10.1029/95RS03817.
Zolesi, B., Belehaki, A., Tsagouri, I., Cander, L.R., 2004. Real-time updating of the simplified ionospheric regional model for operational applications. Radio Sci. 39, RS2011. http://dx.doi.org/10.1029/2003RS002936.
Zuccheretti, E., Tutone, G., Sciacca, U., Bianchi, C., Arokiasamy, B.J., 2003. The new AIS-INGV digital ionosonde. Ann. Geophys. 46 (4), 647–659.